

**Hen 3-160 – the first symbiotic binary with Mira variable S star**C. Gałań<sup>1</sup>, J. Mikołajewska<sup>1</sup>, B. Monard<sup>2</sup>, K. Hkiewicz<sup>1</sup>, D. Pieńkowski<sup>1</sup>,  
and M. Gromadzki<sup>3</sup><sup>1</sup>Nicolaus Copernicus Astronomical Center, Polish Academy of Sciences, Bartycka 18,  
PL-00-716 Warsaw, Poland  
e-mail: cgalan@camk.edu.pl<sup>2</sup>Kleinkaroo Observatory, Calitzdorp, Western Cape, South Africa<sup>3</sup>Warsaw University Astronomical Observatory, Al. Ujazdowskie 4, PL-00-478, Warsaw,  
Poland*Received October 9, 2018*

## ABSTRACT

Hen 3-160 is reported in Belczyński et al.'s (2000) catalog as a symbiotic binary system with M7 giant donor. Using  $V$ - and  $I$ -band photometry collected over 20 years we have found that the giant is a Mira variable pulsating with 242.5-day period. The period-luminosity relation locates Hen 3-160 at the distance of about 9.4 kpc, and its Galactic coordinates ( $l = 267.7^\circ$ ,  $b = -7.9^\circ$ ) place it  $\sim 1.3$  kpc above the disc. This position combined with relatively high proper motions ( $pm_{RA} = -1.5 \text{ mas yr}^{-1}$ ,  $pm_{DEC} = +2.9 \text{ mas yr}^{-1}$ ; Gaia DR2) indicates that Hen 3-160 has to be a Galactic extended thick-disc object. Our red optical and infrared spectra show the presence of ZrO and YO molecular bands that appear relatively strong compared to the TiO bands. Here we propose that the giant in this system is intrinsic S star, enriched in products of slow neutron capture processes occurring in its interior during an AGB phase which would make Hen 3-160 the first symbiotic system with Mira variable S star.

**Key words:** *Stars: abundances - Stars: binaries: symbiotic - Stars: evolution - Stars: late-type - Stars: individual: Hen 3-160*

**1. INTRODUCTION**

The star Hen 3-160 (other designations: SS73 9, WRAY 15-208, Schwartz 1; 2MASS 08245314-5128329) is a symbiotic binary included in the Allen (1984), Kenyon (1986), and Belczyński et al. (2000) catalogs of symbiotic stars (SySt).

According to the Astrophysics Data System (ADS) it was first included in the list of H $\alpha$  emission objects in the southern Milky Way by Wray (1966, table 15), however, it was not bracketed together with zirconium 'S' stars. Sanduleak & Stephenson (1973) included the object in the list of stars in the Southern Milky Way with strong emission lines. They noted Z-And-like emission line spectrum

with sharp He II (4686 Å) and strong hydrogen emissions with an addition of weak He I and forbidden nebular lines and proposed it to be a candidate for SySt. Its SySt nature was soon confirmed by Allen (1978) who described the system as very high-excitation SySt with very strong He II (4686 Å), H $\beta$ , [Fe VII], [Ca VII], and [Ar X] emission lines. Henize (1976) included this object in his catalog of emission-line stars based on its H $\alpha$  emission. Schwartz (1977) also noted the presence of numerous Balmer emission lines in Hen 3-160 spectrum.

There were attempts to detect the object in X-ray or radio waves, but no positive detection was obtained in either case, not in X-rays with ROSAT (Bickert et al. 1996), nor in radio domains (Wright & Allen 1978; Wendker 1995).

Based on analysis of 2MASS photometry by means of  $(J - H) - (H - K_S)$  diagram, Phillips (2007) confirmed the classification of this star to the S-type<sup>1</sup> SySt. Based on near-infrared colors, Allen (1982) divided all SySt into two main classes: (i) most ( $\sim 80\%$ ) belong to a group which near-infrared spectra are generally dominated by the cool star's photosphere, and are indistinguishable from ordinary late-type giants (designated 'S' – for stellar); (ii) the remaining ( $\sim 20\%$ ) SySt exhibit the presence of additional emission due to circumstellar, thick dust shells (D-type). From near-*IR* photometric monitoring, it is known that D-type SySt show large amplitude variations that result from the presence of Mira variables – since they must accommodate the Mira with its dust shell, the orbital periods in these cases should be as long as decades.

Although Hen 3-160 was included in a number of works on large samples of stars characterized with emission features, it has been never subjected so far to any detailed studies and a little is known about the parameters of its components. In this work, we present new observations collected over two decades which enabled us to reveal its very interesting nature. In particular, using our long-term *V*- and *I<sub>C</sub>*-band photometry and optical spectra together with all available near-*IR* measurements we show here that the giant in this system is intrinsic S star, enriched in products of slow neutron capture processes (s-process) occurring in its interior during an AGB phase. This makes Hen 3-160 probably the first known SySt with Mira variable S star.

## 2. Observations and Reductions

Optical spectra were obtained with SpUpNIC spectrograph (Crause et al. 2016; Crause et al. 2018 – in preparation) operated on 1.9 m 'Radcliffe' telescope in Sutherland (South African Astronomical Observatory) during two observing seasons in March 2016 and October 2017. Two gratings (5 and 11) were used to obtain spectra in regions around the H $\alpha$  line ( $\lambda \sim 5950 - 7150$  Å,  $R \sim 3900$ ), and around

---

<sup>1</sup>Historical precedent has resulted in two uses of S for late-type stars. S stars have an overabundance of s-process elements and typically C/O  $\sim 1$ . S-type ('stellar') symbiotic binaries are systems that lack dust.

the Ca II triplet ( $\lambda \sim 7100 - 9700 \text{ \AA}$ ,  $R \sim 2200$ ), respectively. Additionally, we have an older spectrum obtained in November 2005 with the same telescope but equipped with previously mounted Cassegrain spectrograph (SpCCD). This spectrum covers whole optical region ( $\sim 3800 - 7200 \text{ \AA}$ ) in significantly lower resolution ( $R \sim 1000$ ).

Table 1

Journal of spectroscopic observations obtained with 1.9 m telescope at SAAO with information on the acquisition and exposure times, spectral ranges, resolution, spectrograph with which they were acquired, and the measured radial velocities.

Date	HJD	Phase <sup>a</sup>	Spectral Reg.	Spectrograph	Exp. time	Res. pow.	RV
yyyy mm dd	-2450000		[ $\text{\AA}$ ]		[sec.]	$\lambda/\Delta\lambda$	[km/s]
2005 11 20	3694.573	0.031	3810–7220	SpCCD	$3 \times 300$	$\sim 1000$	+109
2016 03 16	7464.411	0.575	5950–7050	SpUpNIC	$5 \times 300$	$\sim 3900$	–
2016 03 20	7468.460	0.592	7150–9700	SpUpNIC	$5 \times 400$	$\sim 2200$	+114
2017 10 22	8048.614	0.984	6050–7150	SpUpNIC	$12 \times 60$	$\sim 3900$	+116
2017 10 30	8056.612	0.017	7100–9700	SpUpNIC	$5 \times 200$	$\sim 2200$	+109

<sup>a</sup> Pulsation phase according to ephemeris:  $\text{JD}_{\text{max}} = 2457810.0 + 242.53 \times E$  (see: Section 3)

All the spectra were reduced, extracted, wavelength calibrated, heliocentric corrected, and calibrated into relative fluxes by standard procedures using *IRAF*<sup>2</sup> packages. The Journal of all spectroscopic observations is shown in Table 1.

Photometric, optical observations of Hen 3-160 in *V* filter were collected during a 20-year period – since November 22, 1997 (JD 2450775.4) till November 17, 2017 (JD 2458074.57) – with a 35 cm Meade RCX400 telescope in Kleinkaroo Observatory equipped with an SBIG ST8-XME CCD camera. Since November 1, 2012 (JD 2456232.60) *I<sub>C</sub>* filter was also included for the monitoring. Each single data point is the result of several individual exposures, that were calibrated (dark-subtraction and flat-fielding) and stacked selectively. Magnitudes were derived from differential photometry to nearby reference stars using the single image mode of AIP4 image processing software. Hen 3-160 was also monitored with the All Sky Automated Survey (ASAS, Pojmański 1997) in *V* photometric band since November 27, 2000 (JD 2451875.74) up to February 20, 2009 (JD 2454882.77). *V* and *I<sub>C</sub>* light curves are shown in Figure 1.

We also used a number of brightness measurements from the literature and published catalogs (Appendix: Table 7). 2MASS All-Sky Catalog of Point Sources (Cutri et al. 2003) gives *JHK* magnitudes obtained on JD 2451140.8321. Kenyon et al. (1988) collated IRAS photometry of SySt providing values of fluxes (in Jy)

<sup>2</sup>IRAF is distributed by the National Optical Astronomy Observatories, which are operated by the Association of Universities for Research in Astronomy, Inc., under a cooperative agreement with the National Science Foundation.

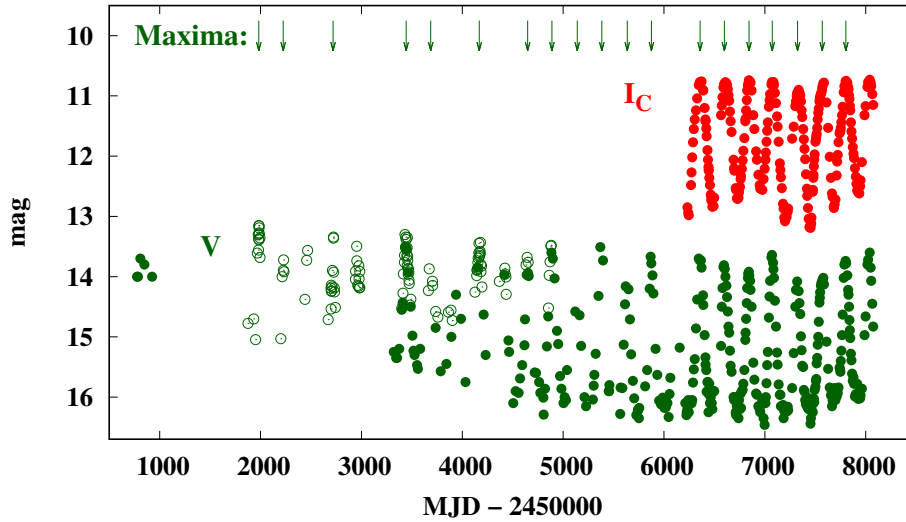


Fig. 1.  $V$  and  $I_C$  light curves of Hen 3-160. Observations obtained at the Kleinkaroo Observatory (solid points) are complemented with the ASAS data (circles). With arrows are shown the moments of pulsation maxima identified and measured in the  $V$  light curve (Section 3).

for Hen 3-160 at  $12\ \mu\text{m}$  and upper estimates for IRAS bands at a longer wavelength. Using NASA/IPAC Infrared Science Archive<sup>3</sup> we extracted infrared photometry from new space infrared missions. AKARI/IRC Point Source Catalogue contain one measurement at  $9\ \mu\text{m}$ . From AllWISE Source Catalog we extracted magnitudes in  $W1$ – $W4$  photometric bands. Additionally, we extracted 55 photometric measurements in total from AllWISE Multiepoch Photometry Table that were made around three dates  $\sim\text{JD } 2455341$ ,  $\sim\text{JD } 2455528$  and  $\sim\text{JD } 2455531$  – these are collected in Appendix: Table 8.

### 3. Pulsational variations of Mira star

$V$ -band photometric data set (complemented with ASAS data) was used for Fourier's analysis which was performed using the discrete Fourier transform method in the Period 04 program (Lenz & Berger 2005). The resulting power spectrum is presented in Figure 2. We derived the value of pulsation period ( $P_{\text{pul}}$ ) and time  $T_0$  corresponding to pulsation maximum at the zero epoch ( $E=0$ ) with which the ephemeris for the maxima of stellar pulsation can be written as follows:  $\text{JD}_{\text{max}} = 2457813.8 + 242.53 (\pm 0.14) \times E$ . The resulting  $T_0$  value is artificially shifted – it clearly does not fall on the pulsation maximum – presumably due to asymmetrical (sawtooth-like) shape of a pulsational light curve. Moreover, the Monte Carlo method implemented in Period 04 program to calculate errors results in severely underestimated error of  $T_0$  – the obtained value of  $\pm 0.03$  is unrealistically small. Phase dispersion minimalization (PDM) analysis (Fig. 2 – bottom) gives period

<sup>3</sup>IRSA (NASA/IPAC Infrared Science Archive), <http://irsa.ipac.caltech.edu/frontpage/>

244 days. In both cases of the power spectrum and PDM similar period being a multiple of pulsation period is obtained and some aliases are present as well as strong noise at low frequencies.

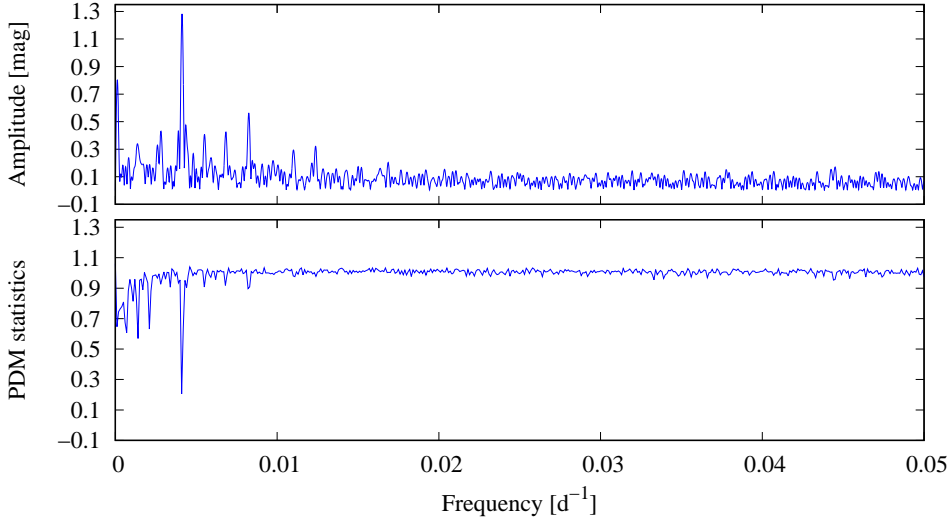


Fig. 2. Power spectrum (*top*) and PDM window (*bottom*) obtained using Fourier's analysis.

Since the Fourier's method was insufficient to obtain a realistic value for time  $T_0$ , we carried out additional analysis of  $O - C$  (observations minus calculations) diagram performed on 19 moments of maxima identified in the  $V$  light curve (Figure 1) which enable to get credible zero point of the ephemeris. The times of maxima were obtained by fit of the second order polynomial (parabola) to the data and are listed in Table 2 together with  $O - C$  residuals in respect to ephemeris obtained with use of Fourier's method and in respect to the new ephemeris with improved  $T_0$  point:  $JD_{\max} = 2457810.0 (\pm 2.2) + 242.70 (\pm 0.17) \times E$ . For the final ephemeris we adopt the zero point ( $T_0$ ) resulting from the  $O - C$  analysis and the period resulting from Fourier's method which uses all points from the light curve and thus should result in more accurate value of the period.

$$JD_{\max} = 2457810.0 (\pm 2.2) + 242.53 (\pm 0.14) \times E.$$

Both,  $V$  and  $I_C$  light curves folded with pulsation period according to the above ephemeris are shown in Figure 3.

It is worth noting that all other observations – both photometric and spectroscopic – in cases when a time of observations is known, show changes correlated with the pulsation phase, eg. WISE photometry in  $W1$ - and  $W2$ -bands shows small amplitude variations in line with the trend of brightness changes in the  $V$  and  $I$  light curves (Appendix: Table 8).

Table 2

Pulsation maxima and the  $O-C$  residuals calculated according to the initial ephemeris obtained with Fourier's method (column 3) and the new ephemeris resulted from  $O-C$  analysis (column 4).

Epoch no.	JD-2450000	$O-C$ [d]	$O-C$ [d]
-24	1982.57	-10.47	-2.71
-23	2224.63	-10.94	-3.35
-21	2718.95	-1.68	5.58
-18	3443.50	-4.72	2.04
-17	3686.23	-4.52	2.07
-15	4168.20	-7.61	-1.35
-13	4648.36	-12.51	-6.59
-12	4888.43	-14.97	-9.21
-11	5139.76	-6.17	-0.58
-10	5383.68	-4.78	0.64
-9	5635.43	4.44	9.70
-8	5874.88	1.36	6.45
-6	6358.50	-0.08	4.68
-5	6599.16	-1.95	2.64
-4	6842.55	-1.09	3.33
-3	7073.14	-13.03	-8.78
-2	7324.74	-3.96	0.13
-1	7569.50	-1.73	2.19
0	7803.14	-10.62	-6.87

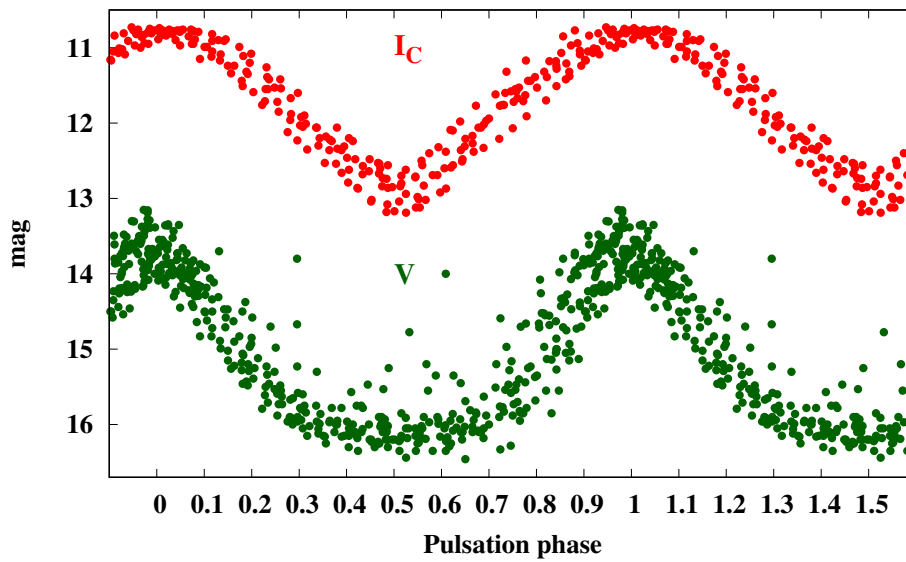


Fig. 3.  $V$  and  $I_C$  light curves folded with pulsation period.

#### 4. Distance and position in the Galaxy

Using known infrared magnitudes and relations binding them with parameters of Mira stars, we can estimate the distance to Hen 3-160 and hence its position in the Galaxy. The period-luminosity relation for O-rich Galactic Miras

$$M_K = -3.51(\pm 0.20) \times (\log P - 2.38) - 7.25(\pm 0.07) \quad (\text{Whitelock et al. 2008})$$

gives the absolute  $K$  magnitude of the Mira in Hen 3-160,  $M_K = -7.27 \pm 0.07$  for  $P = 242.5$  d, with the error inferred from the Whitelock et al relation (note that the error in the period is very small error of order half of permille). Using near- $IR$  photometry from 2MASS and DENIS in  $J$  and  $K$  bands (Appendix: Table 7) we obtain the average  $\bar{K} = 7.81 \pm 0.03$  and  $(J - K) \sim 1.47$ . The intrinsic period-color relation for Oxygen Miras

$$(J - K)_0 = 0.71(\pm 0.06) \times \log P - 0.39(\pm 0.15) \quad (\text{Whitelock et al. 2000})$$

gives  $(J - K)_0 = 1.30$  and hence  $E_{J-K} \sim 0.17$  what is more or less consistent with the total Galactic  $E_{J-K} = 0.26 \pm 0.02$  derived with using the maps of the Galactic extinction by Schlafly & Finkbeiner (2011). The reddening corrected  $K$  magnitude is then  $K_0 = 7.60 \pm 0.11$ , and the **distance to Hen 3-160 is  $d = 9.4 \pm 1.4$  kpc** what remains in perfect agreement with the value of 9.5 kpc estimated by Harries & Howarth (1996). The Galactic coordinates ( $b = -7.87^\circ$ ,  $l = 267.6767^\circ$ ) would then result in  $z = 1.3 \pm 0.2$  kpc which combined with high proper motions ( $\mu_\alpha \cos \delta = -1.504 \pm 0.079$  mas yr $^{-1}$ ,  $\mu_\delta = +2.940 \pm 0.082$  mas yr $^{-1}$ ) from Gaia DR2 (Gaia Collaboration 2016, 2018) suggests that Hen 3-160 could be a Galactic halo object. Using  $M_K = -7.27 \pm 0.07$  and  $BC_K = 3.03 \pm 0.28$  we estimate  $M_{\text{bol}} = -4.24 \pm 0.35$  and thus luminosity  $L = 3960(+1510/-1090)L_\odot$ .

Gaia DR2 gives for Hen 3-160 a negative parallax ( $-0.043 \pm 0.040$  mas yr $^{-1}$ ) with goodness-of-fit statistic parameter  $\text{gofAL} \sim 23$ , that indicates a very poor fit to the data. Bailer-Jones et al. (2018) adopted a special method for estimating distances from Gaia DR2 data, which allows obtaining this information even with the use of negative values of parallaxes. They obtained for Hen 3-160 the distance 12.5 kpc placed in the asymmetric confidence interval from 9.7 to 16.3 kpc which overlaps with the distance derived here using the  $M_K$  magnitude. Our distance would correspond to the parallax  $0.106_{-0.014}^{+0.019}$  mas yr $^{-1}$ . This value is by a factor of  $\sim 30$  smaller than the proper motion from Gaia DR2 and is of the order of its error. Consequently, uncertainty in the parallax cannot bring more than  $\sim 3 - 4\%$  of the proper motion value to the error of this parameter and is irrelevant from the point of view of current considerations.

The Galactic coordinates, distance, and proper motions together with systemic velocity ( $\gamma = 112 \pm 2$  km/s) estimated from measured radial velocities (Table 1) enabled us to estimate Galactic velocities ( $U = -150.3$ ;  $V = -107.5$ ;  $W = +3.3$  km/s).

The obtained values place the system in the extended thick-disc (see eg. Feltzing et al. 2003 – figure 1).

### 5. Changes in spectra and temperature

Based on TiO-bands strength in the near infrared region Mürset & Schmid (1999) estimated the spectral type M7 for the cool component. An infrared domain is particularly useful for studying properties of cool components in SySt as they dominate this spectral range and contribution from the hot component is usually negligible. Mürset & Schmid used spectra obtained at JD 2448696 and JD 2449473, which correspond to pulsation phases  $0.42 \pm 0.04$  and  $0.62 \pm 0.04$  (according to our ephemeris), respectively. Our spectra covering this region (around Ca II triplet) are obtained at  $\phi = 0.017 \pm 0.010$  (October 30, 2017) and  $\phi = 0.592 \pm 0.011$  (March 20, 2016). The first one is placed almost exactly at the pulsation maximum, the second very close to pulsation minimum. Therefore, it is possible to evaluate the range of the Mira spectral type changes due to pulsations by comparing these spectra with those of M-type giant standards. We have the spectra for above a dozen of such M giant spectroscopic standards (Feast et al. 1990; Schulte-Ladbeck 1988) that were acquired during the same seasons as those for Hen-3 160 with the same instrument in identical configuration and thus in exactly the same resolution.

Table 3

Spectral classification of Hen 3-160 based on the strength of TiO band heads in the spectra obtained with SpUpNIC spectrograph (Grating no. 11).

Date yyyy mm dd	Phase <sup>a</sup>	TiO band head ( $\lambda$ [Å]).					Adopted
		7589	8194	8432	8859	9209	
2016 03 20	$0.592 \pm 0.011$	>M4.5	M7.5	>M7.5	>M7.5	>M7.5	>M7.5
2017 10 30	$0.017 \pm 0.010$	M3.5	M4.5	M4	M3.5	–	M3.5–M4

<sup>a</sup> Pulsation phase according to ephemeris:  $JD_{\max} = 2457810.0 + 242.53 \times E$

The method analogous to that applied by Mürset & Schmid (1999) was used to evaluate the spectral type in two approaches:

(i) the strengths of TiO features in the spectra of Hen 3-160 were compared with those in the M giant standard spectra (Figure 4 – left). For each observed depth of TiO band the most suitable spectral type was assigned (see Table 3).

(ii) by dividing the spectrum of Hen 3-160 with the standard spectrum and assessing the smoothest ratio (Figure 4 – right).

For the spectrum from March 2016, the depth of TiO band at 7589 Å indicates the spectral type later than M4.5 while the depths of TiO bands at longer wave-



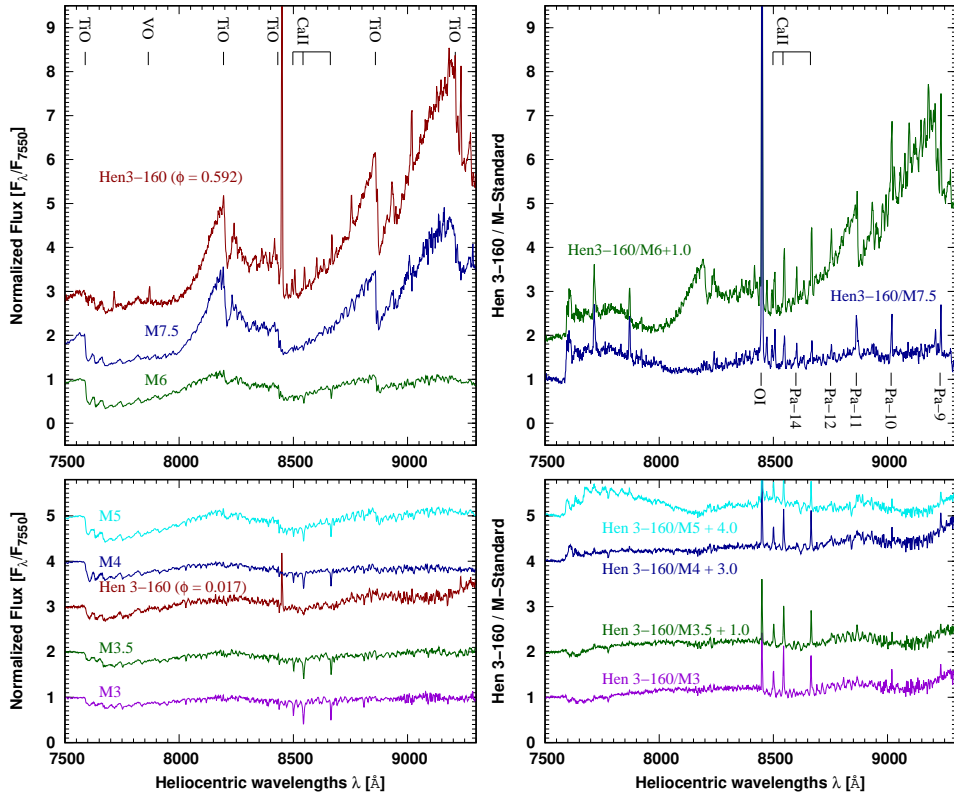


Fig. 4. *Left*: the spectra of Hen 3-160 (red) are compared with the spectra of M-type giant spectroscopic standards (HR 4902, HR 6832, HR 8582, HR 587, HR 7625, and SW Vir) that represent spectral types from M3 to M7.5.

*Right-top*: ratios of the Hen 3-160 spectrum obtained on March 2016 around pulsation minimum with the spectra of standards of types M6 and M7.5 are presented. The nebular contribution is manifested by line emission from Ca II triplet, O I  $\lambda$  8442.36 and numerous HI Paschen series lines.

*Right-bottom*: ratios of the Hen 3-160 spectrum obtained on October 2017 with the spectra of standards from type M3 up to M5.

The spectra are shifted by 1.0 for clarity.

lengths indicate type M7.5 or later (Table 3). This spectrum was placed close to pulsation minimum, where the contribution from a continuum of the hot component must be significant and all these bands must be shallowed, particularly at the blue edge. The division by spectral standards of various types gives the best result for type M7.5, however, it can be seen from Figure 4 (right-top) that a better result should be obtained for the later type:  $>M7.5$ .

For the spectrum from October 2017, the spectral types from the depths of TiO band heads are in the range M3.5–M4.5 (Table 3). The division of this spectrum by the spectral standards (see Figure 4 – right-bottom) indicates that the spectral type between M3.5–M4 should be the most suitable. This spectrum was obtained close to the pulsation maximum phase, i.e. at the condition when the depths of

absorption features including TiO bands were at the least degree influenced by any additional companion light, and it should best pin down Mira’s spectral type. In addition, the temperature of the pulsating giant reaches the maximum value soon before the photometric maximum thus the spectral type derived here represents the lower limit, i.e., it corresponds to the highest expected value of temperature for this star.

Table 4

Spectral type classification performed so far for Hen 3-160.

Date yyyy mm dd	JD/HJD –2400000	Phase <sup>a</sup>	Spectral Region	Spectral Type	Ref
?	?	?	2 $\mu$ m	M7	[1]
1992 03 14	48696	$0.42 \pm 0.04$	6900 – 10700 $\text{\AA}$	M7	[2]
1994 04 30	49473	$0.62 \pm 0.04$	6300 – 10300 $\text{\AA}$	M7	[2]
1994 05 6-10	49479-49483	0.65 – 0.67	6600 – 7400 $\text{\AA}$	M4 <sup>b</sup>	[3]
2016 03 20	57468.4597	$0.592 \pm 0.011$	7150 – 9700 $\text{\AA}$	$\gtrsim$ M8	This work
2017 10 30	58056.6118	$0.017 \pm 0.010$	$\sim$ 7100 – 9700 $\text{\AA}$	M3.5–M4	This work

<sup>a</sup> Pulsation phase according to ephemeris:  $\text{JD}_{\text{max}} = 2457810.0 + 242.53 \times E$ .

<sup>b</sup> This classification has to be mistaken as it was based on the optical spectrum obtained in pulsation phase close to brightness minimum when the absorption features were strongly veiled by the nebular component, and thus imitating earlier spectral type.

**References:** [1]Allen (1980), [2]Mürset & Schmid (1999), [3]Harries & Howarth (1996).

Concluding, the **giant in Hen 3-160 changes its spectral type with the pulsation phase from about M3.5 during the brightness maximum up to M8 (or later) during the minimum.** In Table 4 the values obtained from our spectra are compared with previous results of spectral type classification taken from the literature based on the spectra obtained at various phases. Using the spectral type – effective temperature calibrations (Richichi et al. 1999; van Belle et al. 1999) we obtain the range of temperature changes from  $\sim 3500$  to  $\lesssim 3000$  K. Colors derived from DENIS ( $\overline{J-K_0} \sim 1.16$ ) and 2MASS ( $J-K_0 \sim 1.33$ ) measurements also obtained at phases close to pulsation extrema (DENIS:  $\phi = 0.934$  and  $0.105$ ; 2MASS:  $\phi = 0.502$ ) result in temperatures  $\sim 3550$  and  $\sim 3200$  K respectively.

## 6. Chemical properties of the atmosphere

The strong nebular continuum present in most cases in the optical spectra of SySt causes a decrease in the molecular bands depth, imitating earlier spectral types and lower abundances. This usually causes severe difficulty in studying parameters and measuring abundances of symbiotic giants based on optical spectra. The example can be the spectrum of Hen 3-160 taken on March 2016 close to pulsation

minimum of Mira (Figure 5), which was dominated with radiation from nebula and absorption features completely disappeared. However, in two cases of spectra acquired close to pulsation maximum, the influence by the nebula is already much smaller and absorption features are pronounced. In Figure 5 these spectra (obtained on October 2017 and November 2005) are compared with the spectrum of well known symbiotic S star CD-27°8661 and the normal giant of M3.5 spectral type. The ZrO bands (eg. with the heads at 6342, 6378, 6473, 6495, and 6505 Å) are very clear with strength comparable to those present in the spectrum of S star. In addition, the shape of strong TiO band at  $\sim 6148$  Å is changed in characteristic the s-process enhanced stars way: its head is modified by overlapping YO and ZrO bands. According to the well known spectral classification scheme for cool giants we can ascribe MS spectral type to this object as we see relatively strong ZrO bands in addition to strong TiO bands in its spectrum (compare Hen 3-160 spectra from 2017 and 2005 in Figures 4 and 5 with figure 1 from Yao et al. 2017).

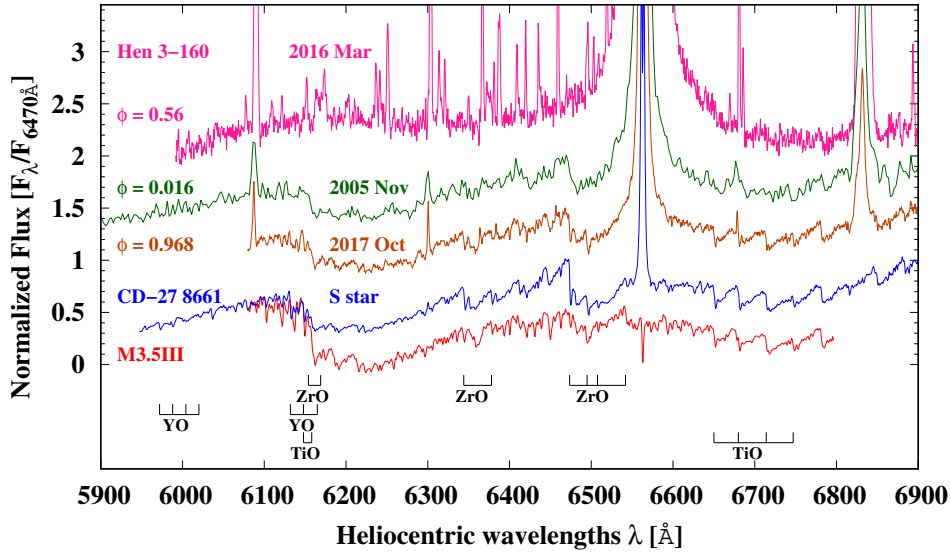


Fig. 5. Comparison of spectra of Hen 3-160 obtained at three various phases – one close to pulsation minimum and two close to pulsation maximum – with the spectrum of well known symbiotic S star CD-27°8661 and a red giant of M3.5 spectral type.

The above confrontation with the spectrum of S star leaves no doubts that the giant in Hen 3-160 is enhanced in s-process elements. As the cool component in Hen 3-160 is a Mira star any quantitative analysis would be problematic because the appropriate atmosphere models do not exist. Nevertheless, we can use our optical spectra with well visible ZrO bands for the analysis of the spectral indices. We performed analysis for a large sample of spectra collected for above 50 symbiotic

giants and a dozen single red giants. The method was similar to that used by Van Eck et al. (2017) in their study of the properties and atmospheres of S stars. We also used their sample of S stars. The band-strength indices were calculated according to the equation:

$$B_X = 1 - \frac{\int_{\lambda_{B_i}}^{\lambda_{B_f}} F_\lambda d\lambda}{(\lambda_{B_f} - \lambda_{B_i})} \frac{\lambda_{C_f} - \lambda_{C_i}}{\int_{\lambda_{C_i}}^{\lambda_{C_f}} F_\lambda d\lambda},$$

where ' $F_\lambda$ ' is the observed flux in the range of wavelength ( $\lambda, \lambda + d\lambda$ ), and indexes 'i' and 'f' denote the wavelengths of beginnings and ends, respectively, of the band 'B' and the continuum 'C' windows listed in Table 5.

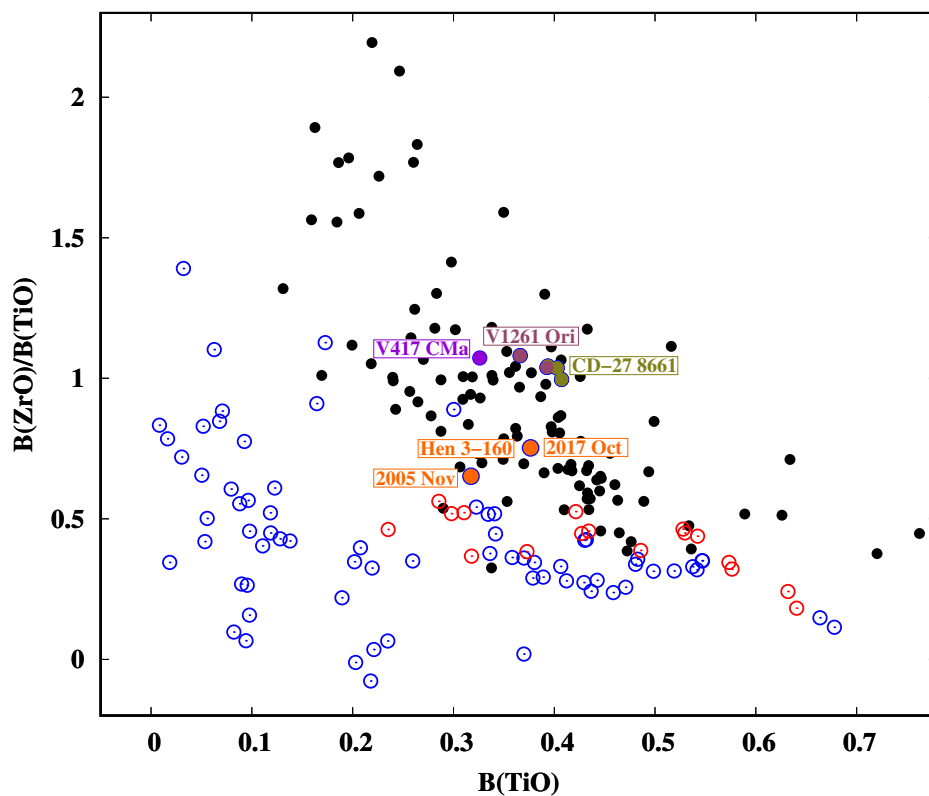


Fig. 6. The plane of indices  $B_{ZrO}/B_{TiO}$  vs.  $B_{TiO}$  with our program SySt (blue circles) and normal M giants (red circles) compared to S stars (black dots). With various coloured circles are distinguished the more interesting cases: well known SySt containing S stars (V1261 Ori, CD-27°8661), suspected SySt with S-type giant V417 CMa, and the positions of Hen 3-160 are featured with orange circles.

The  $B_{ZrO}/B_{TiO}$  vs.  $B_{TiO}$  plane is shown in Figure 6. The indices calculated from the spectrum of Hen 3-160 obtained on October 2017 (at  $\phi = 0.984$ ) result in a position (orange circle) well in the region of S stars, and close to positions of known SySt containing S stars (V1261 Ori, CD-27°8661) and suspected SySt with S-type giant V417 CMa. This is a strong indication that the **giant in Hen**

Table 5

Bands borders that have been adopted to calculate the spectral indices  $B_X$  according to the above formula.

$\lambda_i$	$\lambda_f$	Band	$\lambda_i$	$\lambda_f$	Band
6144.0	6147.5	Cont	6464.0	6472.0	Cont
6148.5	6151.5	TiO	6344.4	6346.0	ZrO
6158.2	6167.8	TiO	6378.0	6379.9	ZrO
6173.7	6181.3	TiO	6473.5	6476.7	ZrO
6185.4	6198.7	TiO	6496.1	6497.4	ZrO
			6507.6	6510.2	ZrO

**3-160 is s-process enhanced star.**

### 7. Spectral energy distribution (SED) analysis

The SED was constructed using all available photometry (Appendix: Table 7). The data was de-reddened using the color excess value  $E_{B-V} = 0.35$  and by adopting the mean interstellar extinction curve for  $R=3.1$  (Fitzpatrick 2004).

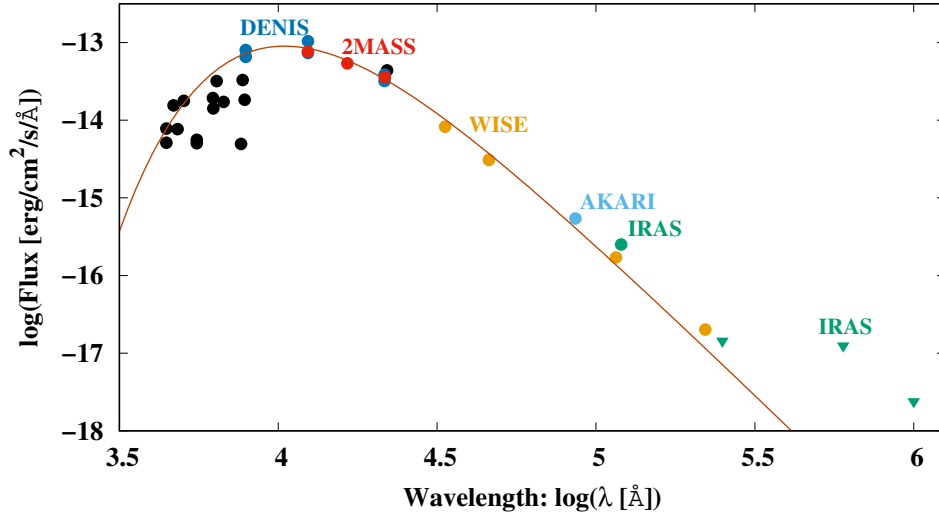


Fig. 7. Spectral energy distribution of Hen 3-160 obtained from all available photometry (Appendix: Table 7). The line shows the fit of Black-Body ( $T = 2770 \pm 330$  K) to the data of the near-*IR* region. Triangles denote the upper estimates.

The magnitudes were transformed into fluxes  $F_\lambda$  expressed in units of [ $erg\ cm^{-2}\ s^{-1}\ \text{\AA}^{-1}$ ] using the Bessel et al. (1998) calibration. Conversion from magnitudes into fluxes  $F_J$  (expressed in Jy) in the case of WISE photometry was made with a

use of zero magnitude flux densities according to Jarrett et al. (2011). Jansky's  $F_J$  were finally recalculated into  $F_\lambda$  fluxes according to the expression:  $F_\lambda = F_J \lambda^{-2} 33356.4095^{-1}$ . The resulted SED is shown in Figure 7 with a fit of Black-Body of temperature  $T = 2770 \pm 330$  K to the data of the near-IR region. **The infrared excess is practically absent which indicates the lack of developed circumstellar dust shell** and confirms the classification of Hen 3-160 as an S-type SySt. This is more or less consistent with theoretical studies by Vassiliadis & Wood (1993) who found out that for Miras with pulsation period below  $\sim 600 - 800$  days the mass-loss rate increases exponentially, while above these values it is essentially constant at the radiation-pressure-driven limit, and at extremely long periods the stars are permanently obscured by circumstellar dust. Our Mira with relatively short  $P_{\text{pul}}=242.5$  d should not be significantly obscured by dust in agreement with the lack of infrared excess observed in the SED. The confrontation with IRAS photometry of SySt (Kenyon et al. 1988) shows that Hen 3-160 has very low infrared fluxes with lack of IR excess – like S-type SySt (which have very low infrared fluxes and in majority only the upper limits are estimated) – and on the contrary to D-type SySt with Mira variables as the cool companion that show significant infrared excesses.

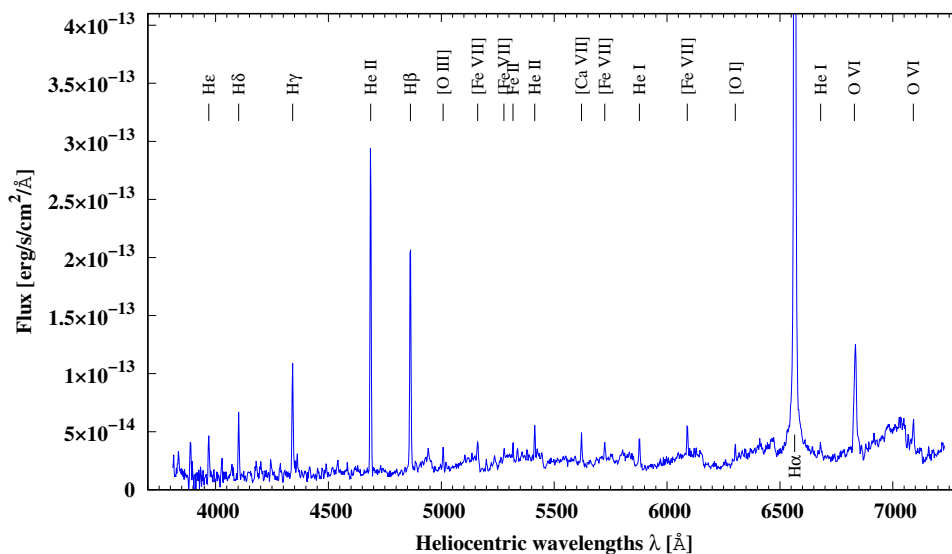


Fig. 8. The flux calibrated, rescaled with  $V = 13.9$  mag and de-reddened the optical spectrum (obtained on November 2005) with identified emission lines marked with ticks.

## 8. The nature of the hot companion

We have observed a number of emission lines in our optical spectra which we use here to shed more light on the nature of the hot component in Hen 3-160 by estimating its temperature and luminosity. We analyzed two spectra obtained

on November 20, 2005, and March 16, 2016. We have applied an absolute flux scale to the first spectrum using the  $V = 13.9$  mag corresponding to the date of its observation ( $V$  light curve – Sections 2 & 3) such that convolution of the spectrum with the Johnson  $V$  filter agrees with the  $V$  mag. The spectrum was de-reddened adequately to  $E_{B-V} = 0.35$ , and the emission line fluxes were measured using *splot* tool of the *IRAF* packages. The identified emission lines are shown in Figure 8 and together with measured flux values are listed in Table 6. The second spectrum was obtained in higher resolution at Mira’s minimum brightness and it was possible to identify a slightly larger number of emission lines. However, it covered too narrow wavelength range to enable the absolute flux calibration using available photometry, and because it does not show the presence of lines corresponding to higher ionization potential it was omitted in the further analysis.

Table 6

Emission line fluxes measured from the spectrum obtained on November 2005 which was de-reddened and scaled to  $V = 13.9$  mag. Ionization potentials are also shown on the right. The errors in the measured fluxes come mainly from uncertainty in the flux calibration of the spectrum which results from scaling with  $V$ -band photometry and are of order 20%.

Line	Measured wavelength $\lambda$ [Å]	Flux [ $10^{-14} \text{ erg s}^{-1} \text{ cm}^{-2}$ ]	$IP$ [eV]
H $\epsilon$	3969.9	24	
H $\delta$	4102.4	33	
H $\gamma$	4341.3	66	
He II $\lambda$ 4686	4686.9	173	54
H $\beta$	4862.9	138	
[O III] $\lambda$ 5007	5008.0	11	55
[Fe VII] $\lambda$ 5158	5161.1	9.9	99
[Fe VII] $\lambda$ 5276	5277.5	3.9	99
Fe II $\lambda$ 5317	5317.4	5.0	16
He II $\lambda$ 5412	5413.8	15	54
[Ca VII] $\lambda$ 5619	5621.0	14.5	109
[Fe VII] $\lambda$ 5721	5723.9	8.3	99
He I $\lambda$ 5876	5877.6	19	25
[Fe VII] $\lambda$ 6086	6089.8	17	99
[O I] $\lambda$ 6300	6302.4	7.9	14
H $\alpha$	6565.4	1249	
He I $\lambda$ 6678	6680.1	8.0	25
O VI $\lambda$ 6825	6825.1	10	114
O VI $\lambda$ 6825	6834.0	105	114
O VI $\lambda$ 7088	7091.0	18.5	114

We used the relation  $T \sim 10^3 \times IP$  (eV) proposed by Mürset & Nussbaumer (1994) to estimate the lower limit of temperature. The method is valid for  $T < 150$  kK. The maximum ionization potential  $IP = 114$  eV is provided by O VI lines

what corresponds to value  $T \gtrsim 114$  kK. The upper limit can be estimated by using the Iijima (1981) method based on the ratios of emission line fluxes of H $\beta$ , He II  $\lambda 4686$  and He I  $\lambda 5876$ . This method is valid for effective temperatures between 70 and 200 kK. The line flux for the line He I  $\lambda 4471$  which originally occurs in the Iijima (1981) equation was replaced here with the flux for the significantly stronger He I  $\lambda 5876$  line taking into account the difference in intensity by a factor of  $\sim 2.7$  (see e.g. Osterbrock 1989). The resulted value of upper limit for WD temperature, in this case, is  $T \lesssim 200$  kK. To estimate luminosity of hot component we used several empirical formulas provided in the literature. The equation 8 of Kenyon et al. (1991) applicable to fluxes from mentioned above three emission lines gives the value of luminosity  $L \sim 770 L_{\odot}$ . Fluxes from He II  $\lambda 4686$  and H $\beta$  lines could be used to estimate luminosity via equations 6 and 7, respectively, of Mikołajewska et al. (1997). We derived the values  $L(\text{He II } \lambda 4686) \sim 1280 L_{\odot}$  and  $L(\text{H}\beta) \sim 1020 L_{\odot}$  for the maximum limit of WD temperature  $T = 200$  kK. All the above estimates adopt the distance to Hen 3-160  $d=9.4$  kpc (Section 4), assume a blackbody spectrum for the hot component and Case B recombination for the emission lines, and have an uncertainty by a factor of two. The comparison with the largest so far studied sample of symbiotic hot components (Mikołajewska et al. 1997) locates Hen 3-160 among the hottest and moderately luminous systems.

## 9. Conclusions

We performed the first comprehensive analysis of the Hen 3-160 symbiotic binary based on new photometric and spectroscopic data in optical and infrared domains. The large-amplitude periodic variations observed in the optical  $V$  and  $I_C$ -band light curves with  $P_{\text{pul}} = 242.5$  days, correlated with changes in other bands as well in the spectra, indicate that the cool component is a Mira star. The changes in the spectral type in the range  $\sim \text{M3.5} - \gtrsim \text{M8}$  estimated based on the TiO bands in optical spectra are correlated with the Mira pulsations.

From the period-luminosity relation, the distance to Hen 3-160 is of about 9.4 kpc. The Galactic coordinates place it  $\sim 1.3$  kpc above the disc and combined with relatively high proper motions indicates that Hen 3-160 has to be a Galactic extended thick disc object.

Our optical spectra show the presence of ZrO and YO molecular bands that are relatively strong compared to TiO bands. The presence of comparably strong ZrO and TiO bands is consistent with the MS spectral type for this object. Analysis of the spectral indices constructed using ZrO and TiO bands has placed Hen 3-160 among the S stars proving that it is enhanced in the s-process elements. To our knowledge, Hen 3-160 is the first known symbiotic Mira that is simultaneously the s-process enhanced star of MS spectral type.

The Mira in Hen 3-160 with relatively short pulsation period should not be significantly obscured by dust which is consistent with very low infrared excess



observed in the SED.

Based on analysis of emission lines in optical spectra the temperature of the white dwarf is in the range of  $\sim 114 - 200$  kK and its luminosity is between  $\sim 770-1280 L_{\odot}$ .

**Acknowledgements.** CG has been financed by the Polish National Science Centre (NCN) grant SONATA No. DEC-2015/19/D/ST9/02974. KI has been financed by the Polish Ministry of Science and Higher Education Diamond Grant Programme via grant 0136/DIA/2014/43 and by the Foundation for Polish Science (FNP) within the START program. This study has been supported in part by NCN grant OPUS 2017/27/B/ST9/01940. MG is supported by the Polish National Science Centre grant OPUS 2015/17/B/ST9/03167. This study uses spectroscopic observations collected with 1.9 m telescope at the South African Astronomical Observatory, which was possible due to Polish participation in SALT funded by grant No. MNiSW DIR/WK/2016/07. This research has made use of the NASA/ IPAC Infrared Science Archive, which is operated by the Jet Propulsion Laboratory, California Institute of Technology, under contract with the National Aeronautics and Space Administration. We would like cordially thank Sophie Van Eck and Alain Jorissen from Université Libre de Bruxelles for providing a rich collection of S stars spectra used in our analysis of the spectral indices.

## REFERENCES

- Allen, D. A. 1978, *MNRAS*, **184**, 601.  
 Allen, D. A. 1980, *MNRAS*, **192**, 521.  
 Allen, D. A. 1982, in: *"The nature of symbiotic stars"*, IAU Coll. No. 95, ed. M. Friedjung and R. Viotti, Astrophysics and Space Science Library, p. 115.  
 Allen, D. A. 1984, *Proc. Astron. Soc. Aust.*, **5**, 369.  
 Altmann, M., Roeser, S., Demleitner, M. et al. 2017, *A&A*, **600**, 4.  
 Bailer-Jones, C. A. L., Rybizki, J., Fouesneau, M. et al. 2018, *AJ*, **156**, 58.  
 Belczyński, K., Mikołajewska, J., Munari, U., Ivison, R.J., & Friedjung, M. 2000, *A&AS*, **146**, 407.  
 Bessell, M. S., Castelli, F., & Plez, B. 1998, *A&A*, **333**, 231.  
 Bickert, K. F., Greiner, J., Stencel, R. E. 1996, in: *"Supersoft X-Ray Sources"*, *Lecture Notes in Physics*, **Vol. 472**, ed. J. Greiner, Springer-Verlag, Berlin, p. 225.  
 Crause, L. A., Carter, D., Daniels, A. et al. 2016, *SPIE – The International Society of Optics and Photonics*, **9908**, 27.  
 Cutri, R. M., Skrutskie, M. F., van Dyk, S. et al. 2003, *VizieR Online Data Catalog: 2MASS All-Sky Catalog of Point Sources (Cutri+ 2003)*.  
 Feast, M. W., Whitelock, P. A., & Carter B. S. 1990, *MNRAS*, **247**, 227.  
 Feltzing, S., Bensby, T., & Lundstrom, I. 2003, *A&A*, **397**, 1.  
 Fitzpatrick, E. L. 2004, in: *"Astrophysics of Dust"*, *ASP Conf. Ser.*, **309**, ed. A. N. Witt, G. C. Clayton, & B. T. Draine, p. 33.  
 Gaia Collaboration; Prusti, T., de Bruijne, J. H. J., Brown, A. G. A. et al. 2016, *A&A*, **595**, 1.  
 Gaia Collaboration; Brown, A. G. A., Vallenari, A., Prusti, T. et al. 2018, *Gaia Data Release 2. Summary of the contents and survey properties*, arXiv:1804.09365G.  
 Girard, T. M., van Altena, W. F., Zacharias, N. et al. 2011, *AJ*, **142**, 15.

- Harries, T. J., & Howarth, I. D. 1996, *A&ASS*, **119**, 61.
- Henden, A. A., Levine, S., Terrell, D., & Welch, D.L. 2015, *American Astronomical Society Meeting Abstracts*, **225**, 336.16.
- Henize, K. G. 1976, *ApJS*, **30**, 491.
- Iijima, T. 1981, in: "*Photometric and Spectroscopic Binary Systems*", ed. E. B. Carling & Z. Kopal, Dordrecht: Kluwer, p. 517.
- Jarrett, T. H., Cohen, M., Masci, F. et al. 2011, *ApJ*, **735**, 112.
- Kenyon, S. J. 1986, "*The symbiotic stars*", Cambridge University Press.
- Kenyon, S. J., Fernandez-Castro, T., & Stencel, R. E. 1988, *AJ*, **95**, 1817.
- Kenyon, S. J., Oliverson, N. A., Mikołajewska, J. et al. 1991, *AJ*, **101**, 637.
- Lasker, B. M., Lattanzi, M. G., McLean, B. J. et al. 2008, *AJ*, **136**, 735.
- Lenz, P., & Breger, M. 2005, *Commun. Asteroseismol.*, **146**, 5.
- Mikołajewska J., Acker A., Stenholm B. 1997, *A&A*, **327**, 191.
- Mürset U., & Schmid H. M. 1999, *A&AS*, **137**, 473.
- Mürset U., & Nussbaumer H. 1994, *A&A*, **282**, 586.
- Osterbrock, D. E. 1989, *Astrophysics of Gaseous Nebulae and Active Galactic Nuclei*, University Science Books.
- Phillips, J. P. 2007, *MNRAS*, **376**, 1120.
- Pojmański, G. 1997, *Acta Astron.*, **47**, 467.
- Richichi, A., Fabbroni, L., Ragland, S., & Scholz, M. 1999, *A&A*, **344**, 511.
- Sanduleak, N. & Stephenson C. B. 1973, *ApJ*, **185**, 899.
- Schlafly E. F., Finkbeiner D. P. 2011, *ApJ*, **737**, 103.
- Schulte-Ladbeck, R. E. 1988, *A&A*, **189**, 97.
- Schwartz, R. D. 1977, *ApJ*, **212**, 25.
- van Belle, G. T., Lane, B. F., Thompson, R. R. et al. 1999, *AJ*, **117**, 521.
- van Eck, S., Neyskens, P., Jorissen, A. et al. 2017, *A&A*, **601**, 10.
- Vassiliadis, E., & Wood, P. R. 1993, *ApJ*, **413**, 641.
- Wendker, H. J. 1995, *A&ASS*, **109**, 177.
- Whitelock, P. A., Marang, F., & Feast, M. W. 2000, *MNRAS*, **319**, 728.
- Whitelock, P. A., Feast, M. W., & van Leeuwen, F. 2008, *MNRAS*, **386**, 313.
- Wray, J. D. 1966, *PhD Thesis*, Northwestern Univ.
- Wright, A. E., & Allen, D. A. 1978, *MNRAS*, **184**, 893.
- Yao, Y., Liu, C., Deng, L., de Grijs, R., & Matsunaga, N. 2017, *ApJSS*, **232**, 16.

## Appendix: complementary tables

Table 7

Photometry taken from the literature and the catalogs, and fluxes calculated as described in section 7.

Band	Wav. $\bar{\lambda}$ [Å]	JD -2450000	Phase <sup>a</sup>	mag	Flux [Jy]	Flux [erg cm <sup>-2</sup> s <sup>-1</sup> Å <sup>-1</sup> ]	Source
Johnson:B	4442	–	–	16.144±0.031		2.13e-15±6.09e-17	APASS DR9 <sup>[1]</sup>
Johnson:B	4442	–	–	16.60		1.40e-15	SPM 4.0 <sup>[2]</sup>
POSS-II:J	4680	–	–	15.18±0.40		4.57e-15±1.72e-15	GSC V.2.3 <sup>[3]</sup>
SDSS:g	4820	–	–	15.816±0.047		2.36e-15±1.02e-16	APASS DR9 <sup>[1]</sup>
Gaia:Gbp	5046	–	–	14.700±0.069		5.86e-15±3.73e-16	Gaia DR2 <sup>[4]</sup>
Johnson:V	5537	–	–	15.640±0.034		1.91e-15±5.99e-17	APASS DR9 <sup>[1]</sup>
Johnson:V	5537	–	–	15.53		2.12e-15	SPM 4.0 <sup>[2]</sup>
Gaia:G	6226	–	–	13.637±0.030		8.53e-15±2.36e-16	Gaia DR2 <sup>[4]</sup>
SDSS:r	6247	–	–	13.954±0.094		6.31e-15±5.47e-16	APASS DR9 <sup>[1]</sup>
POSS-II:F	6400	–	–	12.96±0.44		1.46e-14±6.09e-15	GSC V.2.3 <sup>[3]</sup>
Gaia:G	6730	–	–	13.391±0.036		8.38e-15±2.78e-16	HSONY <sup>[5]</sup>
SDSS:i	7635	–	–	14.154±0.391		2.76e-15±1.02e-15	APASS DR9 <sup>[1]</sup>
Gaia:Grp	7725	–	–	12.041±0.135		1.86e-14±2.32e-15	Gaia DR2 <sup>[4]</sup>
POSS-II:i	7837	–	–	12.61±0.43		1.05e-14±4.27e-15	GSC V.2.3 <sup>[3]</sup>
I	7900	1245.60	0.934	11.191±0.03		3.79e-14±1.05e-15	DENIS
I	7900	1529.79	0.105	10.974±0.02		4.62e-14±8.51e-16	DENIS
J	12390	1140.83	0.502	9.299±0.023		5.98e-14±1.27e-15	2MASS <sup>[6]</sup>
J	12400	1245.60	0.934	9.340±0.04		5.74e-14±2.12e-15	DENIS
J	12400	1529.79	0.105	8.959±0.06		8.16e-14±4.51e-15	DENIS
H	16495	1140.83	0.502	8.333±0.038		4.66e-14±1.63e-15	2MASS <sup>[6]</sup>
K	21600	1245.60	0.934	7.918±0.07		2.93e-14±1.89e-15	DENIS
K	21600	1529.79	0.105	7.712±0.06		3.54e-14±1.96e-15	DENIS
K <sub>S</sub>	21637	1140.83	0.502	7.801±0.021		3.29e-14±6.37e-16	2MASS <sup>[6]</sup>
W1:3.4μm	33500	–	–	7.545±0.036	0.297±0.015 <sup>b</sup>	7.93e-15±4.01e-16	AllWISE SC
W2:4.6μm	46000	–	–	7.268±0.021	0.213±0.008 <sup>b</sup>	3.02e-15±1.13e-16	AllWISE SC
W3:12μm	115600	–	–	6.553±0.016	0.0758±0.0023 <sup>b</sup>	1.70e-16±5.16e-18	AllWISE SC
W4:22μm	220900	–	–	6.018±0.038	0.0327±0.0024 <sup>b</sup>	2.01e-17±1.47e-18	AllWISE SC
2.2 μm	22000	–	–		0.65(∼10%)	4.03e-14±4.03e-15	[7]
9 μm	86100	–	–		0.133±0.008	5.38e-16±3.24e-17	AKARI PSC
12 μm	120000	–	–		0.12	2.50e-16	IRAS <sup>[7]</sup>
25 μm	250000	–	–		<0.03	<1.44e-17	IRAS <sup>[7]</sup>
60 μm	600000	–	–		<0.15	<1.25e-17	IRAS <sup>[7]</sup>
100 μm	1000000	–	–		<0.08	<2.40e-18	IRAS <sup>[7]</sup>

<sup>a</sup>Pulsation phase according to ephemeris:  $JD_{\max} = 2457810.0 + 242.53 \times E$

<sup>b</sup>Calculated with the use of zero magnitude flux densities according to Jarrett et al.(2011)

**References:** <sup>[1]</sup>Henden et al. (2015), <sup>[2]</sup>Girard et al. (2011), <sup>[3]</sup>Lasker et al. (2008), <sup>[4]</sup>Gaia Collaboration (2018), <sup>[5]</sup>Altmann et al. (2017), <sup>[6]</sup>Phillips (2007), <sup>[7]</sup>Kenyon et al. (1988)

Table 8

WISE photometry from AllWISE Multiepoch Photometry Table.

MJD-2450000	phase <sup>a</sup>	W1[mag]	W2[mag]	W3[mag]	W4[mag]
5340.497	0.818	7.446 ± 0.028	7.124 ± 0.026	6.545 ± 0.018	6.113 ± 0.126
5340.761	0.819	7.426 ± 0.021	7.107 ± 0.023	6.545 ± 0.021	5.800 ± 0.077
5340.761	0.819	7.464 ± 0.024	7.161 ± 0.023	6.557 ± 0.018	5.962 ± 0.110
5340.893	0.820	7.426 ± 0.026	7.118 ± 0.020	6.541 ± 0.021	6.076 ± 0.135
5341.026	0.820	7.432 ± 0.025	7.138 ± 0.020	6.535 ± 0.019	6.052 ± 0.096
5341.092	0.821	7.474 ± 0.021	7.110 ± 0.024	6.546 ± 0.016	6.086 ± 0.107
5341.158	0.821	7.454 ± 0.025	7.118 ± 0.019	6.545 ± 0.022	5.875 ± 0.086
5341.224	0.821	7.494 ± 0.027	7.146 ± 0.027	6.553 ± 0.020	6.027 ± 0.095
5341.290	0.822	7.437 ± 0.023	7.134 ± 0.018	6.553 ± 0.019	6.026 ± 0.096
5341.356	0.822	7.427 ± 0.021	7.150 ± 0.020	6.541 ± 0.017	5.858 ± 0.134
5341.423	0.822	7.439 ± 0.023	7.071 ± 0.016	6.555 ± 0.019	5.928 ± 0.097
5341.489	0.822	7.454 ± 0.024	7.144 ± 0.019	6.541 ± 0.019	5.943 ± 0.089
5341.753	0.823	7.492 ± 0.023	7.083 ± 0.019	6.533 ± 0.016	5.943 ± 0.107
5341.819	0.824	7.429 ± 0.020	7.120 ± 0.018	6.574 ± 0.019	6.046 ± 0.096
5341.886	0.824	7.437 ± 0.022	7.151 ± 0.019	6.548 ± 0.016	5.943 ± 0.101
5342.018	0.825	7.423 ± 0.022	7.114 ± 0.016	6.541 ± 0.018	6.134 ± 0.104
5342.084	0.825	7.427 ± 0.021	7.100 ± 0.023	6.594 ± 0.021	6.123 ± 0.100
5342.150	0.825	7.427 ± 0.023	7.095 ± 0.021	6.560 ± 0.019	6.080 ± 0.096
5342.216	0.825	7.444 ± 0.019	7.121 ± 0.018	6.577 ± 0.020	6.202 ± 0.116
5342.283	0.826	7.424 ± 0.023	7.137 ± 0.022	6.561 ± 0.019	6.190 ± 0.110
5342.415	0.826	7.438 ± 0.027	7.159 ± 0.023	6.589 ± 0.023	6.017 ± 0.101
5342.547	0.827	7.436 ± 0.020	7.085 ± 0.018	6.555 ± 0.021	5.972 ± 0.100
5528.462	0.593	7.597 ± 0.045	7.392 ± 0.026	–	–
5528.594	0.594	7.620 ± 0.031	7.341 ± 0.020	–	–
5528.727	0.594	7.682 ± 0.041	7.359 ± 0.022	–	–
5528.859	0.595	7.750 ± 0.043	7.344 ± 0.023	–	–
5528.859	0.595	7.705 ± 0.042	7.337 ± 0.026	–	–
5529.057	0.596	7.702 ± 0.031	7.305 ± 0.017	–	–
5529.124	0.596	7.687 ± 0.031	7.368 ± 0.027	–	–
5530.975	0.596	7.557 ± 0.035	7.356 ± 0.024	–	–
5531.240	0.597	7.637 ± 0.030	7.366 ± 0.028	–	–
5531.306	0.597	7.799 ± 0.055	7.415 ± 0.024	–	–
5531.372	0.597	7.620 ± 0.031	7.350 ± 0.022	–	–
5531.438	0.606	7.629 ± 0.026	7.342 ± 0.021	–	–
5531.504	0.606	7.648 ± 0.037	7.339 ± 0.018	–	–
5531.570	0.606	7.624 ± 0.037	7.348 ± 0.020	–	–
5531.637	0.606	7.642 ± 0.044	7.331 ± 0.023	–	–
5531.703	0.607	7.717 ± 0.036	7.348 ± 0.027	–	–
5531.769	0.607	7.669 ± 0.032	7.394 ± 0.028	–	–
5531.835	0.607	7.705 ± 0.040	7.332 ± 0.021	–	–
5531.901	0.607	7.638 ± 0.038	7.424 ± 0.022	–	–
5531.967	0.608	7.609 ± 0.032	7.404 ± 0.022	–	–
5532.033	0.608	7.753 ± 0.040	7.275 ± 0.021	–	–
5532.100	0.608	7.671 ± 0.035	7.423 ± 0.023	–	–
5532.166	0.609	7.724 ± 0.028	7.321 ± 0.020	–	–
5532.232	0.609	7.737 ± 0.039	7.318 ± 0.021	–	–
5532.232	0.609	7.696 ± 0.031	7.369 ± 0.028	–	–
5532.298	0.609	7.652 ± 0.046	7.343 ± 0.030	–	–
5532.364	0.609	7.671 ± 0.034	7.446 ± 0.022	–	–
5532.430	0.610	7.622 ± 0.033	7.263 ± 0.027	–	–
5532.430	0.610	7.735 ± 0.044	7.384 ± 0.027	–	–
5532.496	0.610	7.641 ± 0.029	7.368 ± 0.023	–	–
5532.629	0.610	7.623 ± 0.058	7.385 ± 0.022	–	–
5532.761	0.611	7.696 ± 0.034	7.360 ± 0.019	–	–
5532.893	0.612	7.661 ± 0.025	7.384 ± 0.015	–	–

<sup>a</sup>Pulsation phase according to ephemeris:  $JD_{\max} = 2457810.0 + 242.53 \times E$